Energy Reports 6 (2020) 3036–3050

Contents lists available at ScienceDirect

Energy Reports

journal homepage: www.elsevier.com/locate/egyr

Sustainable framework for buildings in cold regions of China considering life cycle cost and environmental impact as well as thermal comfort

Ran Wang [a,b], Shilei Lu [a,b,*], Wei Feng [c], Xue Zhai [a,b], Xinhua Li [a,b]

[a] School of Environment Science and Engineering, Tianjin University, 92 Weijin Road, Tianjin, 300072, China
[b] Tianjin Key Laboratory of Built Environment and Energy Application, Tianjin University, Tianjin 300350, China
[c] Lawrence Berkeley National Laboratory, Berkeley, CA 94720, USA

ARTICLE INFO

Article history:
Received 28 April 2020
Received in revised form 16 October 2020
Accepted 17 October 2020
Available online 6 November 2020

Keywords:
Life Cycle Assessment
Life cycle cost
Greenhouse gas emissions
Thermal comfort
Sustainable building

ABSTRACT

In recent decades, environmental problems have enforced designers to estimate the level of environmental emission of building design and reduce their environmental impact. On the premise of ensuring indoor comfort, the cost-effectiveness of solutions for reducing the building's greenhouse gas has become a critical issue. Based on the Life Cycle Assessment (LCA), this paper establishes a building performance trade-off framework for indoor thermal comfort, economics, and environmental implication. This framework consists of four parts: the establishment of the optimization model; sensitivity analysis; obtain of Pareto frontier solutions, and decision-making analysis. Optimization variables involve envelope type and some envelope physical parameters. The "design variables-building performances" database is obtained by using building simulation software combined with the Latin hypercube sampling algorithm. Sensitivity analysis is used to extract the key factors affecting building performance. The designer can prioritize these key factors and it can reduce the uncertainty of building performance. A multi-objective optimization method coupling Gradient Boosted Decision Tree (GBDT) and non-dominated sorting genetic (NSGA-II) algorithm is proposed to seek the trade-off between three performances (obtain Pareto frontier solutions). The Pareto solution provides a more comprehensive reference for the preferences of different stakeholders, and the set of alternative solutions is further shrunk. Finally, take a specific residential building in China's cold climate zone as a showcase of the trade-off framework. According to the obtained Pareto frontier solution, the solution set is shrunk to a certain range, and the distribution ranges of Life Cycle Costs, the greenhouse gas emissions, and the annual thermal discomfort hour ratio are 122.3–137.1 USD/m^2, 15.6–44.8 kg CO_2/m^2, and 19.1–25.2%, respectively. The trade-off framework adopts the order of objective Pareto optimal and then subjective preference selection, narrowing the scope of alternatives for designers and saving time-cost of decision-making.

1. Introduction

According to the International Energy Agency (IEA), the buildings and construction sector accounted for 36% of final energy use and 39% of energy and process-related carbon dioxide (CO_2) emissions in 2018, 11% of which resulted from manufacturing building materials and products such as steel, cement, and glass (IEA, 2019). Given this, some high-performance buildings, including green buildings and zero-energy buildings, emphasize maximum energy conservation and reduce environmental impact. The building design phase has great potential in terms of resource conservation, reduction of energy consumption and environmental impact because decisions at this stage will affect the performance of the building's entire life cycle (Kovacic and Zoller, 2015). The decision at this stage focuses on how to maximize the use of natural resources to decrease the building energy demand and improve occupant comfort. Therefore, it is also called a climate responsive design (Chen and Yang, 2018; Alajmi et al., 2018).

Building design in the early stages is an interdisciplinary issue because its decision-making factors involve an initial investment, building energy consumption, environmental benefits, and thermal comfort. For example, a study compared the environmental impact of four widely used building structures in Central Europe, including reinforced concrete, brick, cross-laminated timber, and

* Corresponding author at: School of Environment Science and Engineering, Tianjin University, 92 Weijin Road, Tianjin, 300072, China.
E-mail address: lvshilei@tju.edu.cn (S. Lu).

https://doi.org/10.1016/j.egyr.2020.10.023

Nomenclature

ACH	Air changes per hour (/hr)
BCAA	The bridge-cutoff aluminum alloy
CEC	The annual cooling energy demand density (kWh/m^{2}a)
CTR	The annual thermal comfort hour ratio (%)
C_o	The annual operation cost (USD/m^{2}a)
CV-RMSE	The coefficient of variation of root mean square error (%)
DCTR	The annual thermal discomfort hour ratio (%)
EUh	hourly heating load (kW)
EUc	hourly cooling load (kW)
E	East
GWP	The greenhouse gas emissions
GBDT	Gradient Boosted Decision Tree
GA	The Genetic Algorithm
HEC	The annual heating energy demand density (kWh/m^{2}a)
HS	Harmony Search
IC	The initial cost (USD/m^2)
LCA	Life cycle assessment
LCC	The life cycle cost (USD/m^2)
LHS	Latin hypercube sampling
MC	Monte Carlo
NSGA-II	The non-dominated sorting genetic
N	North
NMBE	The standard mean deviation
ORNT	Building orientation (°)
PRCC	Partial Rank Correlation Coefficient
PSO	Particle Swarm Optimization
SA	Sensitivity analysis
S	South
Tc	The outdoor temperature (°C)
Tr	The indoor neutral temperature (°C)
USPW	The uniform series present worth factor
WWR	Window to wall ratio
W	West

timber-frame panel construction. The results show that a reasonable choice of components and materials can significantly increase the environmental potential of low-rise buildings (Žigart et al., 2018). Besides, the initial investment is the main reason that hinders the further expansion of markets for high-performance buildings such as zero-energy buildings, especially in developing countries (Feng et al., 2019). The European Union has adopted the cost-optimized design as the main policy requirement for zero-energy buildings. Then this energy policy has driven corresponding scientific research. For example, a study proposed a technology selection framework for new zero-energy buildings based on cost optimization. The results highlight the characteristics of cost-optimized design with climate change. For cold regions, thermal insulation and airtightness are the most important factors (D'Agostino and Parker, 2018). Furthermore, building design is also important for thermal comfort during operation. Due to economic constraints, the HVAC system in China is not open all year round. The building is free-running for several months, and some design parameters have a potential impact on the thermal comfort impact of this period (Wang et al., 2019). Metrics for an optimized building change with different stakeholders. From the government perspective, large-scale reductions in energy consumption and environmental pollution are primary goals. Usually, Developers pay more attention to initial investment. Operating costs and comfort are key considerations for the owner. The proper design should take into account the interests of the government, investors, and owners. But in reality, the passive scheme is usually determined by the architects, while the lack of knowledge about the multidisciplinary expertise results in it is difficult to guarantee optimal application results (Gou et al., 2018).

Decisions during the design phase will affect the entire life cycle of the building, including construction, operation, maintenance, demolition, and use of materials. Life-cycle assessment (LCA) and life cycle cost (LCC) analysis are two commonly used tools to measure the life cycle performance of a product. LCA is a tool for systematically analyzing the environmental impact of products or processes over the various life stages (International Organization for Standardization, 2006). LCC is an economic evaluation technology that covers the total cost of a product including initial investment and operating costs during its life cycle (Mearig et al., 1999). Life cycle analysis has great significance for identifying specific design and decision making improvements in a building (Cabeza et al., 2014; Hurst and O'Donovan, 2019). For example, Jönsson et al. compared the environmental impact of three flooring materials based on LCA and identified solid wood flooring as the most environmentally friendly (Jönsson et al., 1997). Wu et al. discussed the environmental impact of different types of cement and steel on the life cycle (Wu et al., 2005). Islam et al. performed LCA and LCC for typical Australian houses and reported how different roofing and floor designs affect the life cycle environmental impacts and cost (Islam et al., 2015). Schmidt et al. built an integrated framework designed to assist building design professionals in minimizing life cycle greenhouse gas emissions and LCC a building (Schmidt and Crawford, 2018).

Review existing relevant literature, the optimization objectives involved in the issue of building performance optimization can be divided into four categories: energy, economy, environment, and indoor comfort. Energy indicators mainly involved in the existing literature include space heating/cooling energy demand (Harkouss et al., 2018), peak cooling/heating load (Samuelson et al., 2016), and total building energy consumption (Chen and Yang, 2018). Economic indicators mainly involved in the existing literature include initial investment, operating costs, payback period (Wang et al., 2019), and life cycle costs (Mostavi et al., 2017). Environmental indicators are mainly life cycle environmental impact (Glick, 2007)and life cycle carbon emissions (Huang et al., 2012). Comfort indicators mainly include visual comfort (Chi et al., 2018) and thermal comfort (annual comfort time ratio (Gou et al., 2018), utility theory thermal comfort index (Mostavi et al., 2017), the percentage of overheating hours (Harkouss et al., 2018)). However, most research focused on energy indicators, while a small number of studies considered energy and economics or energy and comfort (Shi et al., 2016).

There are always competing relationships between different building performance indicators, such as reduction of energy consumption, financial costs, and environmental impacts. Moreover, the interaction between multi-dimensional design parameters constitutes a complex design space, which results in a lot of data analysis in the optimization process (Lamé et al., 2017). Therefore, the design is a challenging multiple input–multiple output optimization problem. Several studies have performed different mathematical algorithms to solve optimization problems such as the Genetic Algorithm (GA), Particle Swarm Optimization (PSO), and Harmony Search (HS) (Kheiri, 2018). Lu et al. employed a PSO to optimize the various factors (building shape parameter,

envelope parameters, shading system, and courtyard) affecting the energy consumption (Lu et al., 2017). Fesanghari et al. employed an HS based optimization algorithm to determine the best combination of building envelope to minimize the LCC and life cycle carbon emissions (Fesanghary et al., 2012). Ascione et al. employed the genetic algorithm (GA) to determine the best mix of renewable energy for a residential building, aiming to minimize the primary energy demand and investment cost (Ascione et al., 2016). Utilizing artificial neural network-based GA method, Asadi et al. performed a study determined the best retrofit strategies quantitatively, and made a tradeoff between retrofit cost, energy consumption, and hours of occupant discomfort (Asadi et al., 2014). In a word, each of these algorithms uses different strategies to solve a specific range of problems. Compared with other algorithms, GA is more widely used to solve the multi-objective optimization problem in the field of building design.

This article mainly proposes a trade-off framework for building performance that considers economy, comfort, and environmental impact. A specific building layout is selected to showcase this framework. To attain this objective, different construction materials in various building components including the external wall, glazing system, and roof were investigated. Given the interactivity between design variables, some design parameters that have an indirect effect on the optimization goals are also considered. Moreover, the window-ventilation model based on occupant comfort during the transition season is also considered to improve the indoor thermal environment. To solve the multi-objective optimization problem, the GBDT based NSGA-II algorithm is developed and employed. Finally, the optimized framework is applied to a specific type of residential building in the cold climates of China as a display.

2. Method

The main content of this article is to perform sensitivity analysis on the building performance indicators, trade-off analysis of building performance (Pareto frontier solution), and finally decision making analysis. Fig. 1 present the research framework. This section mainly explains the methodology used in the establishment of the framework. Sections 2.1 to 2.3 present the establishment of the optimization model. Section 2.4 describes the Latin Hypercube sampling method and the sensitivity analysis method. Section 2.5 describes the optimization method including GBDT meta-models technology and NSGA-II optimization algorithm.

2.1. The optimization variables

Table 1 shows the optimization variables and their distribution for the cold climate zone. To meet the energy-saving goals, the range of several envelope performance parameters is imposed mandatory in building design standards. Generally speaking, it should be satisfied in the building design. In this paper, the optimization variables mainly refer to the constraints of building design standards and the level that market technology can achieve. According to the "Design Standards for Energy Conservation of Residential buildings in Cold and Cold Regions" (Ministry of Construction P R China, 2010), for a three-story building, the U-value of the external wall and the roof cannot be higher than 0.45 W/(m^2 K) and 0.35 W/(m^2 K). On the other hand, according to the field investigation, the lower limit of the U-value achieved by increasing the insulation is 0.1 W/(m^2 K). Therefore, the range of the external wall and roof is 0.1–0.45 W/(m^2 K) and 0.1–0.35 W/(m^2 K), respectively. Besides, the maximum window-to-wall ratio for different orientations is also stipulated: north, south, west, and east directions are 0.4, 0.6, 0.45, and 0.45 respectively. The range of the U-value and SHGC of the external window also meets the requirements of the design standards. According to various studies on residential buildings and energy codes in China and the EU, the airtightness level should be between 0.5 and 1.5 ACH (Chen et al., 2019). The types of external walls, external windows, and roofs are commonly used in this climate zone based on field investigations. Mention cases of Wall type/Roof type/Window type will be documented later. The design variables can be regarded as being equally probable in building design, they should be defined as uniform distributions when the aim is to identify effective energy-saving measures (Mechri et al., 2010).

The building orientation is also an important factor affecting the heat gain/loss in the building envelope. The direct solar radiation received by different building surfaces varies according to their orientation (Dutta et al., 2017). When considering the trade-offs between energy consumption, cost, and environmental impact, there may be differences in the optimal solutions for external windows of different orientations. For example, in a passive optimization study on new residential buildings in hot summer and cold winter regions in China, according to this study, when the goal is to improve indoor thermal comfort while reducing building energy demand, the U-value ranges of external windows in different orientations in the Pareto front solution is different (Gou et al., 2018). Therefore, this paper distinguishes the external windows of different orientations, but the range is the same.

What needs to be mentioned is that external walls, external windows, roofs, and floors are of the same grade. However, considering the large fluctuations of the outdoor meteorological environment compared to ground temperature, this article mainly focuses on the external windows, roofs and external walls that are in direct contact with the outdoor meteorological environment.

Fig. 2 shows the common practices of exterior walls and roofs by investigating the local actual cases. The base layer of the external wall is the Aerated concrete block, and that of the roof is the Reinforced concrete floor. Table 2 summarized the common type of insulation and window. The four commonly used insulation materials are Rock wool, PU panel, EPS panel, and XPS panel. The thermal characteristics of these building materials are shown in Table 3.

2.2. The assessment indicators

In recent decades, environmental problems have enforced designers to estimate the level of environmental emission of building design and reduce their environmental contribution (Mahapatra, 2015). On the premise of ensuring indoor thermal comfort, the cost-effectiveness of solutions for reducing the building's greenhouse gas has become a critical issue for building owners (Ellis, 2009). Therefore, this article takes the economy, environmental impact, and thermal comfort as optimization objectives. LCC is a commonly used economic evaluation indicator in the building design and construction (Cabeza et al., 2014). The Global Warming Potential (GWP) is a commonly used environmental impact evaluation indicator, which measures how much heat Greenhouse Gas traps in the atmosphere and is expressed in carbon dioxide equivalent (CO2e) (Schmidt and Crawford, 2018). Besides, the annual indoor thermal comfort time ratio (CTR) is a commonly used thermal comfort evaluation indicator (Wang et al., 2019; Gou et al., 2018). Therefore, LCC, GWP, and CTR are used as indicators for the economy, environmental impact, and thermal comfort, respectively.

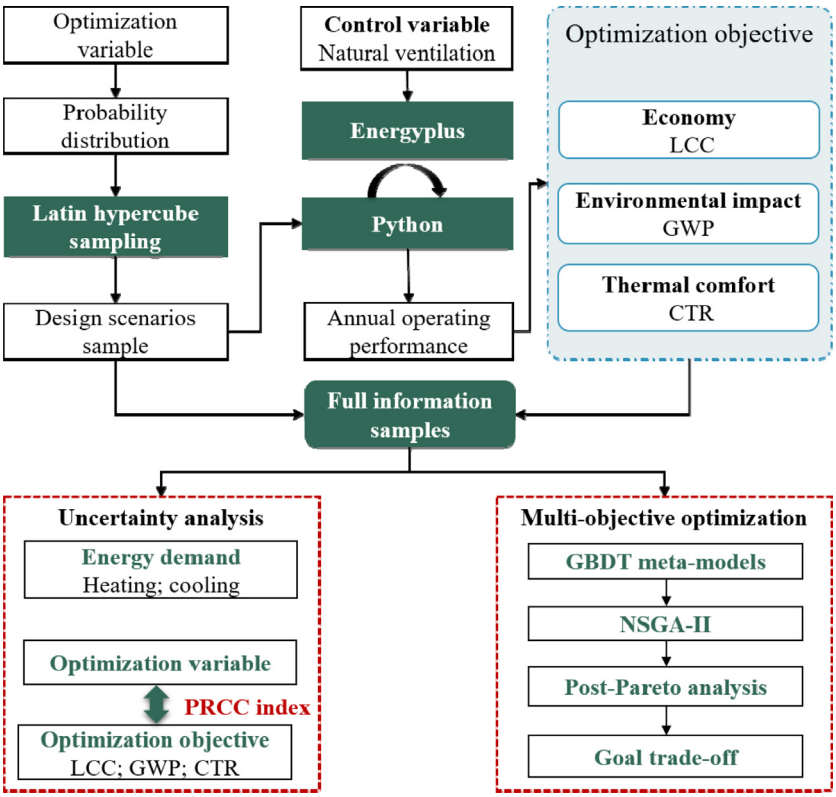

Fig. 1. The research framework.

Table 1
The distribution of thermal performance.

Categories		Parameter	Unit	Probability density functions	Range
Wall		U-value	W/(m^2 K)	Continuous uniform	[0.1,0.45]
Roof		U-value	W/(m^2 K)	Continuous uniform	[0.1,0.35]
Window	N	U-value	W/(m^2 K)	Continuous uniform	[1.2,2.2]
		SHGC	/	Continuous uniform	[0.1,0.45]
	S	U-value	W/(m^2 K)	Continuous uniform	[1.2,2.2]
		SHGC	/	Continuous uniform	[0.1,0.45]
	W	U-value	W/(m^2 K)	Continuous uniform	[1.2,2.2]
		SHGC	/	Continuous uniform	[0.1,0.45]
	E	U-value	W/(m^2 K)	Continuous uniform	[1.2,2.2]
		SHGC	/	Continuous uniform	[0.1,0.45]
WWR		North	/	Continuous uniform	[0.2,0.4]
		South	/	Continuous uniform	[0.2,0.6]
		West	/	Continuous uniform	[0.2,0.45]
		East	/	Continuous uniform	[0.2,0.45]
Airtightness		ACH_{50}	/hr	Continuous uniform	[0.5,1.5]
Orientation (ORNT)		Building north axis	°	Continuous uniform	[0,360]
Wall type		/	/	Discrete	[1,2,3,4]
Roof type		/	/	Discrete	[1,2,3,4]
Window type		/	/	Discrete	[1,2,3]

Table 2
The common type of insulation and window.

Categories	No.	Type
Insulation	1	Rock wool
	2	PU panel
	3	EPS
	4	XPS
Categories	No.	Type
Window	1	Plastic steel+ Double-layer ordinary glass
	2	BCAA +Single layer Low-E glass+Single layer of ordinary glass
	3	Plastic steel +Single layer Low-E glass+ Double-layer ordinary glass

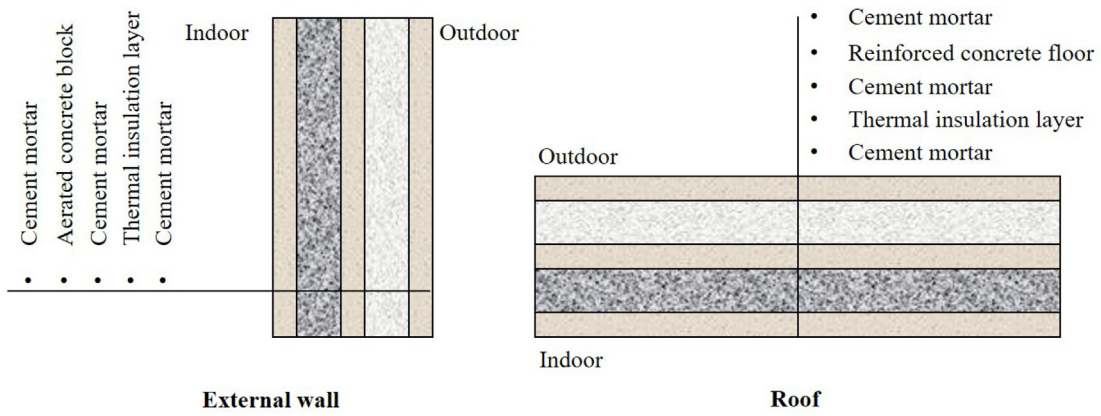

Fig. 2. Schematic of common practices for exterior walls and roofs.

Table 3
Thermal physical properties of building materials.
Source: Ministry of Construction P R China (2016).

Materials	Dry density (kg/m^3)	Thermal conductivity [W/(m K)]	Heat storage coefficient [W/(m^2 K)]	Specific heat capacity [kJ/(kg K)]
Cement mortar	1800	0.93	11.37	1.05
Aerated concrete block	500	0.14	2.31	1.05
Reinforced concrete floor	2500	1.74	17.2	0.92
Rock wool	60∼160	0.041	0.47∼0.76	1.22
PU panel	35	0.024	0.29	1.38
EPS	20	0.033	0.28	1.38
XPS	35	0.03	0.34	1.38

2.2.1. The economic indicator

The LCC is adopted to evaluate the building model's cost-effectiveness. LCC is the most frequent method to estimate the financial benefits of energy conservation projects over their lifetime.

$$LCC = IC + USPW(N, rd) \times C_o \tag{1}$$

$$USPW(N, rd) = \frac{1-(1+rd)^{-N}}{rd} \tag{2}$$

Where USPW is the uniform series present worth factor (it converts future recurrent expenses to present costs) (years), which can be obtained by Eq. (2). The C_o (USD/m^2) represents annual operation cost, which can be obtained by Eq. (3); IC (USD/m^2) stands for the initial cost of implementing design and operating conditions for building envelope, which can be obtained by Eq. (8). The rd is the annual discount rate (%) and N stands for the life period (year). Herein, the life period is set to 30 years (Harkouss et al., 2018; Bichiou and Krarti, 2011). There is a difference between "nominal interest rate" and "real interest rate", that is, (1+real interest rate)=(1+nominal interest rate)/(1+inflation rate). But considering that the future inflation rate is difficult to assess, this article is based on the nominal interest rate, that is, the static discount rate is used. With reference to most previous studies (Harkouss et al., 2018; Bichiou and Krarti, 2011; Ouyang and Lin, 2014), the static discount rate is generally set to 5%. It is worth mentioning that the construction costs of various materials are just indicative due to the potential change in prices in the market.

The C_o is calculated as follows:

$$C_o = C_{heating} + C_{cooling} \tag{3}$$

The operating cost during the heating season ($C_{heating}$, USD/m^{2}a):

$$C_{heating} = (HEC \times HC)/M \tag{4}$$

The operating cost during the cooling season ($C_{cooling}$, USD/m^{2}a):

$$C_{cooling} = (CEC \times CC)/M \tag{5}$$

Among then, HC is the local heating cost, 0.0186 USD/kWh. CC is the electricity price, 0.0716 USD /kWh. M (m^2) is the conditioning area—1029.6 m^2 in this paper. HEC (kWh/a) is the annual heating energy demand and CEC (kWh/a) is the annual cooling energy demand, they can be obtained by Eq. (6) and Eq. (7).

Same as most existing research, the entire building energy consumption is obtained utilizing EnergyPlus software(Ver.9.0.1), which is a highly validated simulation engine widely used in building energy analysis (Crawley et al., 2001). Building energy consumption mainly refers to space heating and cooling energy consumption. Because less affected by the building envelope parameters, domestic hot water, and lighting energy consumption is not considered. According to the actual operating characteristics of local residential buildings, the urban heating network and the household air conditioner is used in the winter and the summer, respectively. The COP value of air conditioning for cooling is 2.8.

The HEC and CEC can be calculated as follows:

$$HEC = \sum_{i=1}^{i=Nh} EU_{hi} \tag{6}$$

$$CEC = \sum_{i=1}^{i=Nc} EU_{ci} \tag{7}$$

The EU_i is hourly energy demand in kWh, which can be obtained through building performance simulation; N_h is annual heating hours, which is 1815 h; N_c is annual cooling hours, which is 1861 h.

The IC is calculated as follows:

$$\begin{aligned} IC &= (E_{roof} + E_{wall} + E_{window})/M \\ E_{roof} &= m_{roof} \times C_{roof} \\ E_{wall} &= m_{wall} \times C_{wall} \\ E_{window} &= m_{window} \times C_{winodw} \end{aligned} \tag{8}$$

Table 4
The unit price of insulation and exterior windows.
Source: China Building Materials Online website. http://www.cnjcw.com/.

Categories	No.	Cost (CNY/m^3)	Cost (CNY/m^2 mm)
Insulation	1	301.6	0.302
	2	680	0.68
	3	348	0.348
	4	501	0.501
Categories	No.	Cost (CNY/m^2 mm)	
Window	1	310	
	2	450	
	3	483	

Among them, m_{roof} is the roof area, which is 343.2 m^2 in this study. m_{wall} and m_{window} are the external wall area and external window area, respectively. Since the window-to-wall ratio is an optimized variable in this study, the external window and wall areas are both variable and related to specific sampling. C_{roof}, C_{wall} and C_{window} represent the unit price of the roof, external wall, and external window respectively. For this study, there are mainly insulation layers of wall and roof as well as external windows that cause differences in initial investment between different alternatives. According to the latest material prices on the China Building Materials Online website (http://www.cnjcw.com/), the prices of commonly used building materials are summarized in Table 4. This cost refers to the price of the insulation layer per unit area and unit thickness. The unit area is "m2" and the unit thickness is "mm". The numbers in the table are the type number of thermal insulation materials and exterior windows. The detailed information is shown in Table 2.

2.2.2. The thermal comfort indicator

It is necessary to specify indoor thermal comfort standards for the design, energy calculations, and building operation. Thermal comfort is "that condition of mind that expresses satisfaction with the thermal environment and is assessed by subjective evaluation" (ASHRAE, 2016). There are many ways to evaluate thermal comfort due to differences in occupants, climate conditions, usage scenarios, and stages of building. In this study, due to the presence of HVAC systems in summer and winter, the indoor thermal environment can be considered comfortable. The evaluation object is mainly the transition season, during which Chinese buildings are generally free-running. The adaptive model can be used to evaluate the thermal comfort of free-running status, and it quantifies the relationship between indoor neutral temperature and the outdoor environment. The ANSI/ASHRAE-55 adaptive model is the most commonly used one that built on the field data from various climate zones (Carlucci et al., 2018).

The neutral temperature calculation based on the ASAHE-55 model is shown in Eq. (9):

$$T_c = 0.31 \times T_r + 17.8 \tag{9}$$

T_c represents the indoor neutral temperature. T_r is the monthly average outdoor temperature, the data of a typical meteorological year are used here and see Table 6 for details. When considering 80% acceptability, thermal comfort fluctuates within 3.5 °C on either side of T_c (7 °C bandwidth). The model applies to an outdoor average temperature between 10 and 33.5 °C.

The upper (T_{upper}) and lower limits (T_{lower}) of the thermal comfort zone are:

$$T_{upper} = T_c + 3.5 \tag{10}$$

$$T_{lower} = T_c - 3.5 \tag{11}$$

In this study, Beijing is used as the case, T_{upper} and T_{lower} are present in Table 6.

Based on the adaptive model, the CTR is used as a thermal comfort measure. The calculation formula is as follows:

$$CTR = \frac{1}{m}\sum_{k=1}^{k=m}\left(\sum_{j=1}^{Np} wf_j \cdot \frac{1}{Np}\right)^m \in [0, 1] \tag{12}$$

$$wf_j = \begin{cases} 1, & if \quad T_{lower} \le T \le T_{upper} \\ 0, & if \quad T \prec T_{lower} \ or \ \succ T_{upper} \end{cases} \tag{13}$$

Where T is the comfort indicator, which here is the indoor operating temperature, which can be obtained through building performance simulation. N_P represents the total hours, which is 3900 h. The m is the number of the thermal zone. Each flat is modeled as a thermal zone, and there are 9 thermal zones in the whole building. For different thermal zones, the indoor thermal comfort level is different. For the convenience of calculation, the average comfort level of nine thermal zones is used to represent the whole building.

Besides, indoor thermal comfort could be totally satisfied during the summer cooling and winter heating periods. The building is free-running in the transition season, so it is a goal to improve the indoor comfort as much as possible by optimizing the passive design of the building. Therefore, the optimization of the annual CTR is actually the optimization of the transition season CTR.

2.2.3. The environmental impact indicator

Some high-performance buildings, such as green buildings, generally stipulate that buildings should maximize energy conservation and emission reduction throughout the life cycle, creating a comfortable and efficient environment for occupants. Therefore, when designing the envelope, attention should also be paid to the environmental impact of building materials throughout the life cycle. The greenhouse gas emission (GWP) is selected as environmental impact assessment indicators.

$$GWP = m_{wall} \cdot GWP_{wall} + m_{roof} \cdot GWP_{roof} + m_{window} \cdot GWP_{window} \tag{14}$$

GWP_{wall}, GWP_{roof} and GWP_{window} are the units GWP for exterior walls, roofs, and exterior windows, respectively.

The unit GWP of commonly used insulation layers and external windows are shown in Table 5. The GWP value of different materials comes from "Green Building Material Selection Technology" (China Building Materials Inspection and Certification Group, 2015), which was jointly published by "China National Building Material Inspection and Certification Group" and "China National Building Materials Testing Center". The GWP values in Table 5 are for the entire external window (including frame and glazing). GWP is an indicator to measure the environmental impact of the envelope material and has nothing to do with the way of opening, mainly varies depending on the window frame and glass material. If window frames and glass are used as the basis for classification, there are three types of external windows involved in this article. No. 1 is a plastic steel window frame + ordinary glass. No. 2 is broken bridge aluminum alloy + Low-E glass + ordinary glass, and No. 3 is plastic steel window frame + Low-E glass + ordinary glass. For different numbers of the same external window type, only the thickness of the air layer is different to obtain various thermal parameters. More detailed physical information about these external windows is shown in Table 2.

2.3. The optimization function

The adopted objective functions in this optimization problem are to minimize LCC and GWP as well as maximize CTR. Hence, the optimization function can be summarized as follows:

$$F(\vec{x}) = \begin{cases} f_1 = f(\vec{x}, LCC)_{\min} \\ f_2 = f(\vec{x}, GWP)_{\min} \\ f_3 = f(\vec{x}, CTR)_{\max} \end{cases} \tag{15}$$

Table 5
The GWP of insulation materials and external windows.
Source: A book called "Green Building Material Selection Technology" (China Building Materials Inspection and Certification Group, 2015), which was prepared by the "China Building Materials Inspection and Certification Group" and the "National Building Materials Testing Center".

Categories	No.	GWP ($kgCO_2/kg$)
Insulation	1	5.02
	2	11.5
	3/4	12.1
Categories	No.	GWP ($kgCO_2/m^2$)
Window	1	9.88
	2	15.25
	3	11.7

Among then, the represent the optimization variables set.

2.4. The statistical method

2.4.1. Sampling method

Most of the optimization variables in this paper are "continuous uniform distribution", and continuous uniform distribution means that each value within the range of the variable has the same probability of being selected. The diversity of design variable values is called the uncertainty of design variables. For design variables that have been assigned a distribution, the sampling method can be employed to obtain a sample of each design variable. Monte Carlo is a widely used method of uncertainty analysis in building performance assessment (Silva and Ghisi, 2014). Moreover, Latin hypercube sampling (LHS) is a stratified sampling method for the Monte Carlo method that divides the range of each input variable into N segments with the same probability distribution. With the same statistical accuracy, the required sample size of LHS is smaller than that of random sampling (Helton et al., 2006). Therefore, LHS is more suitable for complex computational models that contain many uncertain variables. It is generally recommended for the minimum sampling size to be 10 times the number of variables (Levy and Steinberg, 2010).

2.4.2. Sensitivity analysis method

Sensitivity analysis is the science that studies how the uncertainty in the output can be apportioned to the various uncertainties in the input (Pang et al., 2020). In this article, sensitivity analysis is used to extract the influence of design variables on building performance. Commonly used global sensitivity analysis methods include linear regression, Fourier sensitivity analysis, and Sobel sensitivity analysis methods. Since the calculation is fast and easy to understand, the regression method is the most commonly used method (Tian, 2013). Many sensitivity indicators are derived based on regression methods, such as SRC (Standardized Regression Coefficients), PCC (Partial Correlation Coefficients), SRRC (standardized rank regression coefficient), and PRCC (partial rank correlation coefficient). The PRCC is usually used for problems where the input and output are nonlinear and monotonic (Gagnon et al., 2018). PRCC indicators can show the influence level and influence direction of optimization variables on each optimization objective. The influence level is represented by the absolute value of PRCC. The influence direction is indicated by positive and negative signs.

2.5. The optimization method

To reduce the call of programming software to the simulation software and thereby improve the optimize efficiency, the meta-models participate in the optimization process as the fitness function of the optimization algorithm is the main trend (Ostergard et al., 2018). Select the appropriate meta-model construction methods and optimization algorithms are the two keys to multi-objective optimization.

The meta-model in building optimization design refers to using mathematical algorithms to learn the relationship between optimization variables and building performance based on a small amount of data obtained from the simulation software and then constructing a substitute model to predict the building performance. Machine learning algorithms are commonly used methods for building meta-models, including the multiple linear regression (MLR), multivariate adaptive regression splines (MARS), support vector machines (SVM), artificial neural network (ANN), Gradient Boosted Decision Trees (GBDT), etc. For example, a study built meta-models of building performance using ANN and dynamically coupled with the Non-dominated Sorting Genetic Algorithm-II (NSGA-II) to obtain the best trade-off between heating and cooling performance (Bre et al., 2020). In a study on the passive design optimization of high-rise residential buildings in Hong Kong, MLR, MARS, and SVM were employed to develop meta-models (Chen and Yang, 2017). In a previous study on the optimization design of a passive house by the author, GBDT was used to construct meta models of building energy consumption and thermal comfort ratio, and the results proved that GBDT has better robustness and fitting characteristics (Wang et al., 2019). This research continues the previous research and adopts GBDT to develop meta-models. The applicability of model accuracy is generally measured using the standard mean deviation (NMBE) and the coefficient of variation of root mean square error (CV-RMSE), which are specified in ASHRAE Guideline 14-2002. When NMBE and CV-RMSE less than $\pm 5\%$ and $\pm 15\%$, respectively, the meta-model is accurate and reliable (ASHRAE, 2002).

The concept of "optimal" between multi-objective optimization and single-objective optimization problems are different. When dealing with multi-objective optimization problems with multiple conflicting objectives, the idea of Pareto optimal solutions can help the decision-makers decide among the best alternatives (Kheiri, 2018). Pareto optimal when there is not any other feasible solution that improves one objective without deteriorating at least another one. Different non-dominated solutions are identified rather than one optimal solution. The set of best alternatives, Pareto-optimal, is called Pareto-front (Machairas et al., 2014). Therefore, the "Pareto optimal" concept is not equivalent to the common "optimal". Since no weights are given, Pareto optimal is less subjective and fair to all optimization objectives (Deb, 2015). The Pareto solution can be used as a reference for the trade-off between different candidate solutions. After obtaining the Pareto front, it is usually necessary to make further decisions based on different preferences of stakeholders (Harkouss et al., 2018). Early discussions about Pareto optimal in building design optimization can be traced back to 1980 Radford and Gero (Radford and Gero, 1980). Subsequently, the application of Pareto optimal solution in building design became more and more common. For example, in a multi-objective optimization problem on rural tourism buildings in north China, a Pareto frontier solution set considering energy consumption, daylighting, and thermal comfort performance is given (Zhu et al., 2020). Another study proposed a multi-objective optimization method for building renovation. The objectives include energy-demand reduction, energy-cost reduction, investment cost reduction, and CO_2 emissions reduction. The Pareto frontier solution was applied to a residential building in Rome, Italy (Rosso et al., 2020).

In addition, there are often non-linear interactions of building variables on the objectives of building issues, and the properties of these variables may be continuous or discrete (Nguyen et al., 2014). The GA, which belongs to the evolutionary algorithms, has

the advantage of handling both continuous and discrete variables, meanwhile having good robustness for handling discontinuity, multi-modal and highly-constrained problems without trapped into a local minimum. These make GA an effective tool to deal with complex and multivariate building problems (Nguyen et al., 2014). A study counts the optimization algorithms commonly used in the literature on building optimization design, and the results show that there has been a rapid increase in the utilization of GA, considerably higher than the other methods (Kheiri, 2018). There have been also many GA-based algorithms developed to be adapted for different specific problems, among which, the NSGA-II algorithm, developed by Deb (Deb, 2001), has been recognized as one of the most efficient algorithms (Zitzler et al., 2000) and successfully implemented in the field of building performance optimization. For example, Multi-objective optimization of building renovation in the Mediterranean climate (Rosso et al., 2020), energy and daylight optimization of shading devices (Kirimtat et al., 2019), window design considering energy consumption, thermal environment and visual performance (Zhai et al., 2019), and optimization design of low-rise commercial buildings under various climates (Lapisa et al., 2018).

Therefore, this paper uses the GDBT based NSGA-II algorithm to solve the established multi-objective function. The final result in this paper also proves that the method is effective with a set of Pareto solutions that are finally obtained.

2.6. Case study

2.6.1. The base building model

As detailed in previous articles published by the author (Wang et al., 2019), a generic building model (see Fig. 3) is developed in EnergyPlus. The case building is a slab-type apartment, which is the most popular form of residential buildings in China. The rectangular footprint of the total building is 31.2 m×11.0 m (length×width) with three flats of each story. Each flat is modeled to a thermal zone, and there are 9 thermal zones in the whole building. The layer height is 2.9 and the shape coefficient is 0.299. The building long axis is oriented East–West. The internal thermal load from lighting, equipment, and people are assumed to be 4.3 W/m^2 on average. It is assumed that three persons live in each flat, and their schedule of a workday is 16:00 to 8:00 the next day. The using schedule of lighting is 8:00–9:00 and 16:00–23:00; the using schedule of the equipment is 8:00–9:00 and 18:00–19:00. When the iterative simulation is performed for each set of design scenarios, in turn, building geometry and operation are the same, and all building properties not governed by optimization variables are consistent in all models. Considering that during the actual operation of the building, when occupants feel uncomfortable, they may adjust the indoor temperature by opening windows (Yun et al., 2008). The "window-opening model" here is established based on the occupants' thermal comfort, can be used to simulate the window opening behavior of occupants when they are uncomfortable. The adaptive thermal comfort model is used as a metric for opening and closing windows. The external window is openable with the minimum opening angle being 0.3. The establishment of the model refers to the "Input and output reference" file of EnergyPlus (DOE. Documentation Input Output Reference. https://energyplusnet/sites/all/modules/custom/nrel_custom/pdfs/pdfs_v890/InputOutputReferencepdf).

2.6.2. The meteorological condition

The cold climate of China is dominated by heating, and the central heating system is used in winter. According to the design orientation in the existing building standards, the building design features in the climate are mainly thermal insulation in winter, and some areas of the climate zone take into account the heat dissipation in summer (MOHURD, 1993). The main features of the cold climate are: the average temperature in January is −10 to 0 °C, and the average temperature in July is 18 to 28 °C. Select a typical city — Beijing as a representative city. Beijing is located in eastern China (39.8N, 116.47E, and elevation 31.3 m). Its HDD18 and CDD26 are 2794.8 and 70.9 respectively. Typical meteorological year data is used as the meteorological parameter. The T_r, T_{lower} and T_{upper} are presented in Table 6. T_{lower} and T_{upper} are calculated according to Eqs. (10) and (11), respectively.

The division of the heating season, the cooling season and the transition season of the building are determined by combining government policies and the living habits of the local occupants. For the cold climate zone of China, the district central heating is used to maintain indoor comfort in the winter. The heating period is approved by the local government, which is generally from mid-November to mid-March next year. Household air conditioners are used to maintain indoor comfort in summer. Although the cooling period is not restricted by the government, according to the local weather network survey, the cooling period is generally from mid-May to mid-September (The-weather-network. Tianjin's air conditioning opening hours in summer. https://www.tianqi.com/news/145484.html). The period other than the cooling period and heating period is the transition season. Its indoor thermal comfort could be totally satisfied during the summer cooling and winter heating periods. The building is free-running during the transition season, so the indoor thermal comfort cannot be fully guaranteed. During this period, the building mainly relied on the performance of the envelope to adjust the indoor thermal comfort. Therefore, it is the main goal to optimize thermal comfort during this period by adjusting the envelope design parameters.

3. Result and discussions

3.1. Characteristics of energy demand

Fig. 4 shows the distribution of HEC and CEC under the interaction effects of uncertain design parameters and the variation of C_o with HEC and CEC. The horizontal and vertical coordinates are HEC and CEC, respectively, and the unit is "kWh per square meter per year". Points with different colors are used to describe the distribution of C_o, and the unit is "USD per square meter per year". C_o is calculated according to Eqs. (3)–(5), and HEC and CEC are calculated according to Eqs. (6) and (7), respectively. Uncertainty in design variables has less impact on CEC than on HEC with a fluctuation range of CEC and HEC being 34–44 kWh/(m^{2}a), and 5–45 kWh/(m^{2}a), respectively. The CEC exhibits a normal distribution but HEC is relatively average in different frequency bands. Colors are used to represent the size of the C_o value. For example, red and blue represent C_o values of 7.3–7.8 USD/m^2 and 9.5–10 USD/m^2, respectively. Through color mapping, C_o changes with CEC and HEC can be intuitively displayed. As the CEC and HEC increase, C_o gradually increases with a certain slope. CEC contributes the most to C_o.

3.2. Impact of optimization variables on optimization objectives

Fig. 5 shows the PRCC indices for all three optimization objectives. In terms of CTR, almost all optimization variables have an impact on it in addition to ACH, ORNT, roof type, and wall type. Among then, the south-facing WWR is ranked first with PRCC equal to 0.89. Followed by north-facing WWR, south-facing window U-value, south-facing SHGC, north-facing SHGC, north-facing U-value, and wall U-value with PRCC over 0.30. Then, west-facing WWR, roof U-value, east-facing WWR, east-facing window U-value, and west-facing window U-value also have

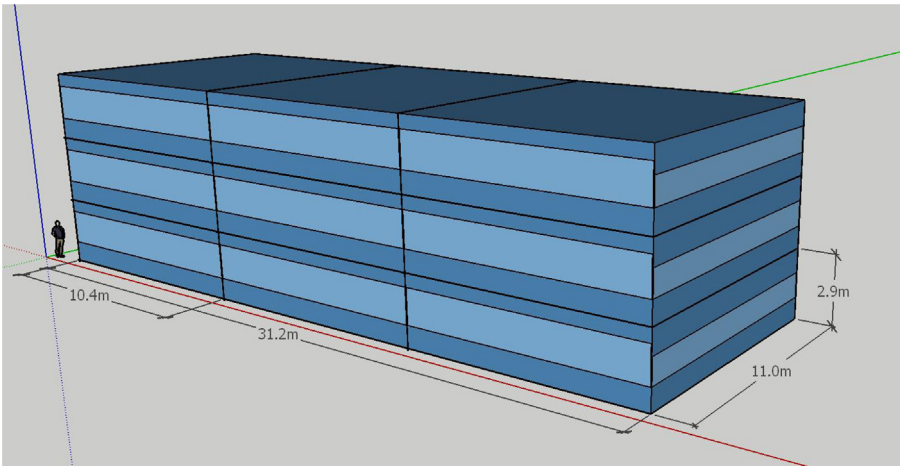

Fig. 3. Elevation and isometric view of base building.

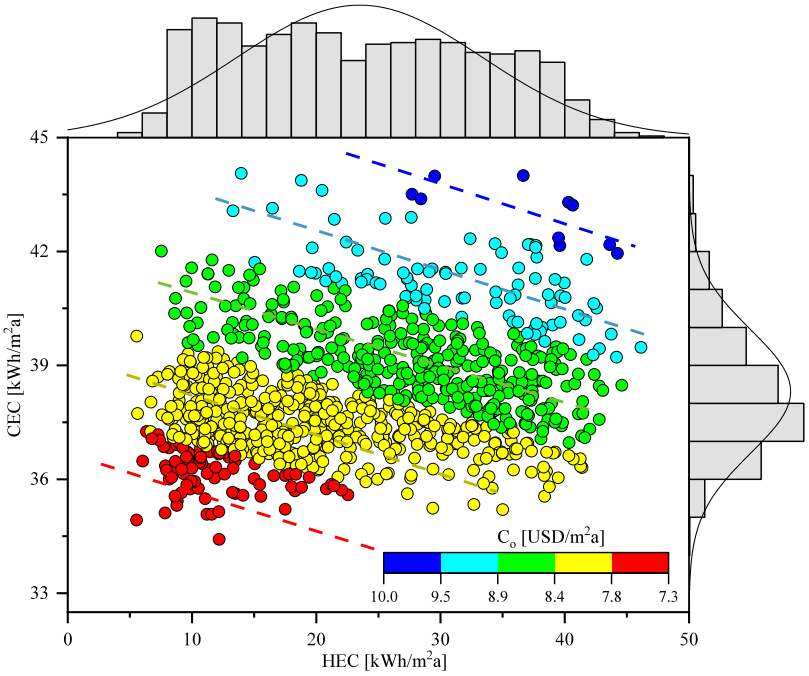

Fig. 4. The distribution of building cooling and heating demand.

Table 6
The T_r, T_{lower} and T_{upper} of Beijing.

The Months	1	2	3	4	5	6	7	8	9	10	11	12
T_r (°C)	16.6	17.3	20.2	22.3	23.8	25.4	26.0	25.7	24.1	21.8	19.5	17.7
T_{lower} (°C)	13.1	13.8	16.7	18.8	20.3	21.9	22.5	22.2	20.6	18.3	16.0	14.2
T_{upper} (°C)	20.1	20.8	23.7	25.8	27.3	28.9	29.5	29.2	27.6	25.3	23.0	21.2

some certain impact with PRCC between 0.1 and 0.3. What needs to be mentioned here is that since the annual CTR is mainly determined by the indoor thermal environment during transition season, it is assumed that window ventilation can be carried out during the transition season, which weakens the impact of airtightness.

In terms of LCC, ACH rank first, then followed by south-facing SHGC, north-facing SHGC, and south-facing WWR. The roof type, wall type, ORNT, west-facing window U-value, and south-facing window U-value almost do not affect LCC with PRCC less than 0.1. In terms of GWP, Only four variables have significant impacts, namely the roof type, roof U-value, the wall type, and wall U-value, especially wall U-value with PRCC equal to 0.72. The remaining variables have little effect on GWP with PRCC less than 0.1.

Compare the differences in the parameter sets that affect the three optimization objectives. The number of variables that have a significant impact on GWP and LCC is less than the CTR. The sign of PRCC represents the overall influence direction of design parameters on optimization objectives. When a design parameter has inconsistent influence direction on all three optimization objectives, it indicates that the design parameter is a trade-off variable. For example, the WWR in all orientations is negatively correlated with CTR and GWP but positively correlated with the

Table 7
The NMBE and CV-RMSE of meta-models.

Indicator	DCTR	GWP	LCC
NMBE [%]	2.63	3.28	1.78
CV-RMSE [%]	3.00	4.52	1.36

Table 8
The setting of the NSGA-II algorithm.

Parameter	Value
Population size	500
The number of maximum generation	2000
Generation gap	0.8
Crossover probability	0.8
Mutation probability	0.6

LCC, moreover, they are more sensitive to CTR than LCC and GWP. The U-value in all orientations negatively correlated with both CTR and LCC, and SHGC in all orientations positively correlated with both CTR and LCC. Besides, CTR is more sensitive to the U-value and SHGC of the external window than LCC with the relatively large absolute value of PRCC. The U-value of both roof and wall is positively correlated with CTR, GWP, and LCC. The ACH has a relatively large impact on LCC but hardly affects GWP and CTR. The main reason is that ACH significantly affects HVAC energy consumption, especially heating energy demand, which in turn affects the LCC.

3.3. The Pareto frontier solution

The optimization model established aimed to improve CTR and reduce LCC as well as GWP. However, multi-objective optimization problems generally refer to optimize either minimum or maximum objectives. Therefore, DCTR minimization is used to represent CTR maximization. Performing the GBDT-based NSGA-II method to solve multi-objective function in Python language.

Based on the GBDT algorithm, meta-models of optimization variables to DCTR, LCC, and GWP are established. According to Fig. 6, there is a better fit performance between the simulated and predicted data value with the R^2 of LCC, GWP, and DCTR being 0.996, 0.998 and 0.991, respectively. Table 7 presents the accuracy measures of various meta-models. The accuracy of meta-models established by the GBDT algorithm for each performance indicator meets the technical requirements with NMBE and CV-RMSE less than $\pm$5% and $\pm$15%, respectively.

In terms of the main parameters in the NSGA-II algorithm, the roulette selection method and two-point cross are selected. The default value of several other important optimization settings, including the population size, number of maximum generations, generation gap, and crossover and mutation probability are summarized in Table 8.

Fig. 7 shows the Pareto frontier solutions when optimizing three objectives at the same time. To visually show the relationship between any two objectives, it is displayed by a 2-D coordinate graph. The distribution ranges of LCC, GWP, and DCTR are 122.3–137.1 USD/m^2, 15.6–44.8 kg CO_2/m^2, and 19.1–25.2%, respectively. Fig. 7(a) shows the mapping of DCTR on the graph of the LCC-GWP plot. When LCC and GWP are the main optimization targets, solutions are concentrated in the frontier, and the boundary is very clear. DCTR has significant changes in both directions "a" and "b", gradually reduced along with the two directions. At the frontier of the LCC-GWP plot, the DCTR of "area A" is minimal. From the "area A" along with the "a" and "b" directions, as well as the direction of "c", the DCTR gradually increases. Fig. 7(b) shows the mapping of the LCC on the DCTR-GWP plot. The LCC has a significant change in the"a" and "b" direction. When in the frontier solution (only for the DCTR-GWP plot), LCC is the largest relative to other solutions. As the GWP decreases, the DCTR increases dramatically along with the direction "a". Fig. 7(c) shows the mapping of GWP on the DCTR-LCC plot. On the whole, the GWP at the frontier is the largest. In the direction of "a", the GWP gradually increases. Comparing Figs. 7(a), (b) and (c), it can be found that when any two optimization targets are used as the analysis object, the third targets of the solution on the forefront is the largest.

Fig. 8 shows the distribution space of optimization variables corresponding to the Pareto frontier solution. The variables are normalized so that the distribution of all variables can be displayed in one figure. The distribution preference of each variable is determined by the level and direction of their influence on each optimization objective. We can use the position of the mean and median to represent the distribution preference. In terms of wall U-value and roof U-value, they prefer to be distributed near the upper limit, especially the roof. This is in contrast to our conventional energy-efficient building design which stipulates that the insulation level should be as high as possible. This is because when the life cycle cost and environmental benefits are taken into account, the reduced operating costs due to the increased insulation are less than the other adverse effects that increase. In particular, the thermal insulation of roofs only has a direct impact on the units on the top floor and has little impact on the entire building, especially high-rise buildings. For external windows, parameters of north-facing and south-facing have more concentrated distributions. The U-value of north-facing and south-facing windows distributed in the middle and SHGC prefer to distribute near the lower limit. For WWR, the south-facing is more concentrated than other orientations. The east-facing and north-facing have no obvious distribution preference being concentrated in the intermediate position. The west-facing and north-facing prefer to the upper limit. ACH prefers relatively small values. The optimal orientation of the Building North Axis concentrated in 130–180°. The optimal type of exterior wall is type 3, that is, EPS is used as the insulation material. Optimized roof types include type 1 and 3, with Rock wool or EPS as insulation material.

3.4. Decision-making analysis

For multi-objective optimization problems, the Pareto frontier solution only provides a set of alternatives rather than any finalized and determined solution, which can provide a reference for decision-makers. Decision-makers can assign weights to the three optimization objectives according to their preferences, and then further refine the solution from the Pareto frontier solution. In short, the Pareto solution is objective, while the decision maker's option is subjective. After obtaining the Pareto frontier solution, it is generally necessary for the designer to decide to obtain a more detailed solution.

This article selects three typical situations from the Pareto front solution for further analysis. That is, decision-makers, prioritize the economy, thermal comfort, and environmental impact respectively. For example, when decision-makers prioritize the economy, the Pareto front solutions are sorted in the order of LCC from small to large, and the minimum LCC is 122.3 USD/m^2. The solution with the smallest LCC among the Pareto frontier solutions can be selected as shown in Fig. 9(a). What needs to be mentioned is that there may be multiple solutions that meet the minimum LCC. Similarly, the smallest DCTR and GWP are 19.1% and 15.6 kg CO_2/m^2, respectively. The solution sets for the smallest DCTR and smallest GWP are shown in Figs. 9(b) and (c), respectively. It can be seen from Fig. 9 that the Knee point under the three decision criteria is point A, point B, and point C, respectively. To visually compare the three cases, these points

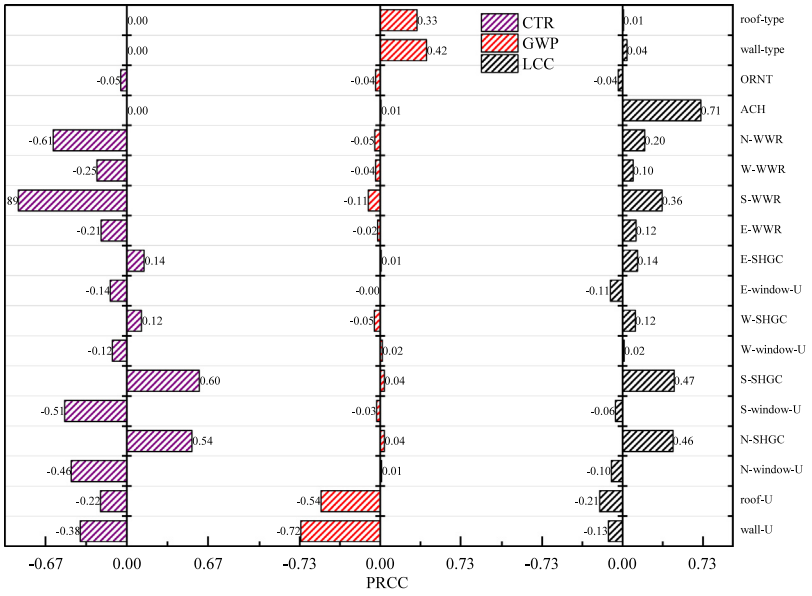

Fig. 5. The result of redundancy analysis.

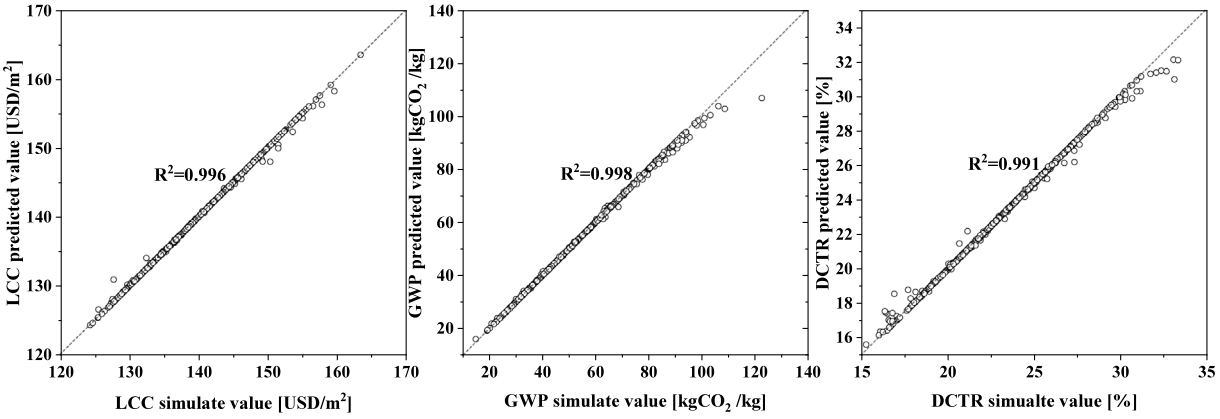

Fig. 6. The fit of simulated values and predicted values based on the GBDT meta-model.

are displayed on the same coordinate axis, as shown in Fig. 10. The X, Y, and Z coordinates are LCC, DCTR, and GWP respectively. The LCC, DCTR, and GWP of point A are 122.3 USD/m^2, 23.6%, and 33.4 kg CO_2/m^2, respectively. The LCC, DCTR, and GWP of point B are 125.3 USD/m^2, 19.1%, and 17.2 kg CO_2/m^2, respectively. The LCC, DCTR and GWP of point C are 133.6 USD/m^2, 22.3% and 15.6 kg CO_2/m^2, respectively. Obviously, point B is closest to the coordinate origin. When comprehensive considering the three optimization objectives, point B is the best choice. The corresponding design schemes of these three points are summarized in Table 9. The WWR, airtightness, external window parameters for north and east between the three points differed slightly. For the three points, the insulation type for both external walls and roofs is almost EPS. The exterior window type on the north, south, and east is type 2 (bridge-cutoff aluminum alloy +Single layer Low-E glass+Single layer of ordinary glass), and the most suitable exterior window form on the west is Type 3 (Plastic steel +Single layer Low-E glass+ Double-layer ordinary glass).

Table 9
The corresponding design schemes of three decision points.

Categories	Point A	Point B	Point C
Wall U-value	0.23	0.40	0.44
Roof U-value	0.23	0.30	0.30
N-U-value	2.19	2.18	2.17
N-SHGC	0.10	0.24	0.10
S-U-value	2.20	1.41	2.20
S-SHGC	0.10	0.30	0.28
W-U-value	1.36	1.27	1.32
W-SHGC	0.14	0.40	0.39
E-U-value	2.20	2.04	2.04
E-SHGC	0.10	0.10	0.10
E-WWR	0.35	0.33	0.32
S-WWR	0.40	0.40	0.40
W-WWR	0.44	0.44	0.44
N-WWR	0.42	0.43	0.45
ACH	0.50	0.54	0.52
ORNT	180.00	20.93	178.29
Wall type	EPS	EPS	EPS
Roof type	Rock wool	EPS	EPS
N-window type	2	2	2
S-window type	2	3	2
W-window type	3	3	3
E-window type	2	2	2

3.5. The limit and future research

The specific building layout limits the generalization possibilities of optimization results. However, it is important to note

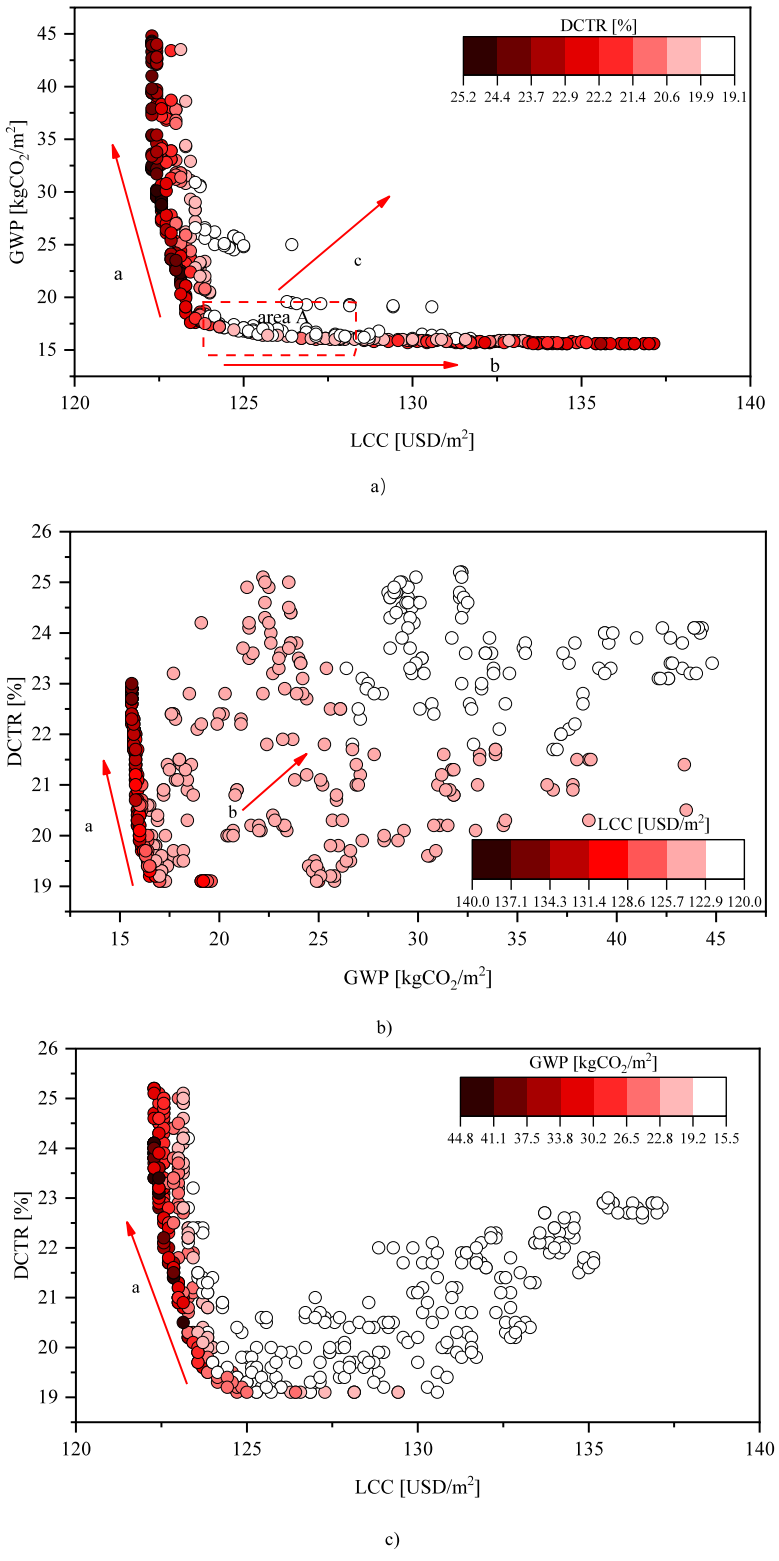

Fig. 7. The Pareto frontier solution targeting minimum LCC, DCTR, and GWP.

that this paper provides a trade-off framework for the apartment building in the cold climate of China. The framework can be extended to various building typology and climate contexts. Besides, the sensitivity analysis results obtained in this study will vary depending on the specific form of the building. For example, the thermal insulation of roofs only has a direct impact on the units on the top floor and has little effect on the entire high-rise buildings.

4. Conclusion

In the early stage of building design, making proper decisions can assist designers to attain the best sustainability. This

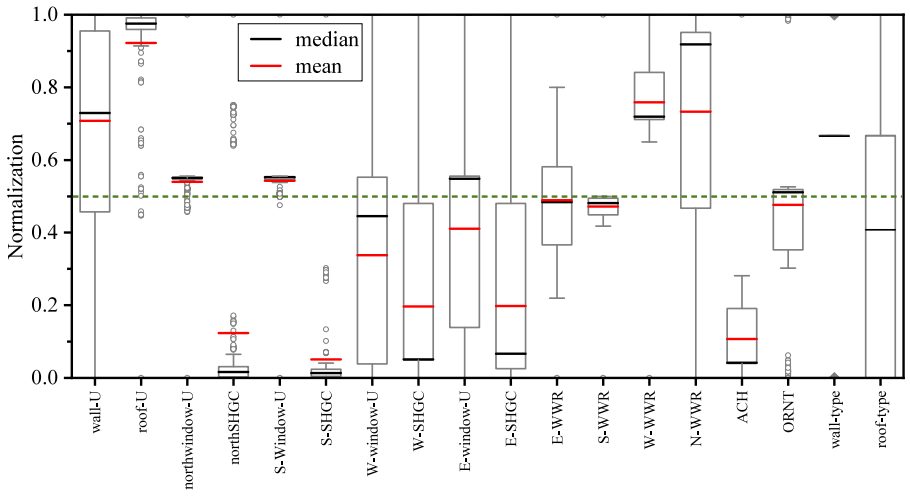

Fig. 8. The corresponding solution set of Pareto frontier solution.

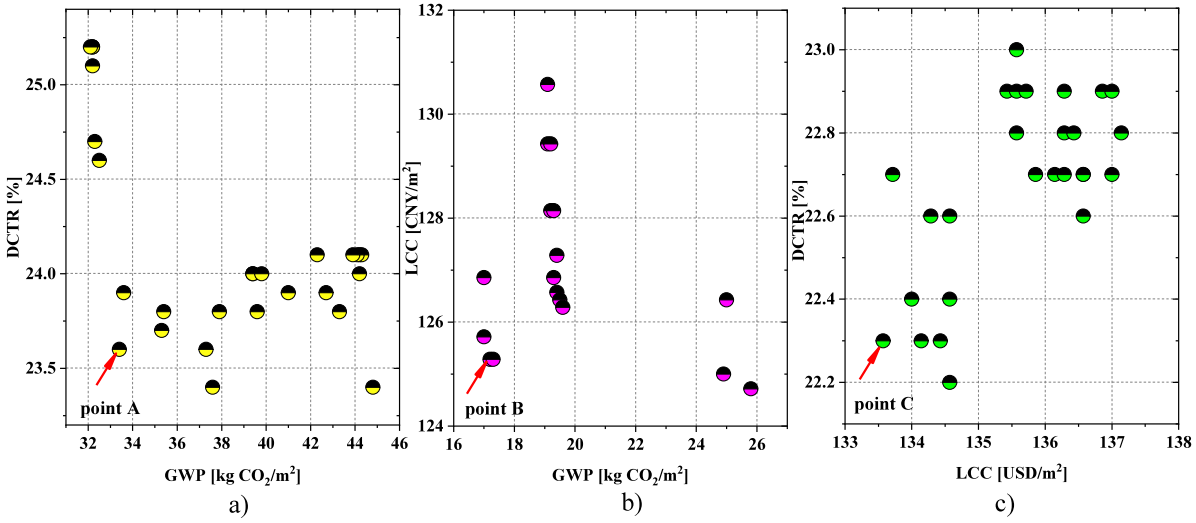

Fig. 9. The decision making (a) With minimum LCC; (b) With minimum DCTR; (c) With minimum GWP.

article establishes a trade-off framework for multiple building performance. Optimization objectives include environmental implication, indoor thermal comfort, and economic benefits. The optimization variables involve envelope type and some key physical parameters. A building information database is generated by employing simulation software and the Latin hypercube sampling methods. The trade-off framework is mainly composed of three parts: sensitivity analysis, Pareto optimization, and decision making analysis. The sensitive analysis method is used to identify and compare the key factors affecting each optimization objective. These key factors should be given priority in the building design stage. It can reduce the uncertainty of building performance and thereby reduce the decision-making difficulty of designers. Then, the multi-objective optimization method based on the coupling of the meta-model technology and genetic algorithm is used to obtain the Pareto frontier solution. This set of Pareto frontier solutions can provide a more comprehensive reference for the different stakeholders. Stakeholders can weight the optimization objective according to their preferences, and then extract the final solution from Pareto solutions.

To visually demonstrate the working process of the trade-off framework, it is applied to a specific residential building in cold climate zones of China. According to the obtained Pareto frontier solution, the solution set is shrunk to a certain range, and the distribution ranges of Life Cycle Costs, the greenhouse gas emissions, and the annual thermal discomfort hour ratio are 122.3–137.1 USD/m^2, 15.6–44.8 kg CO_2/m^2, and 19.1–25.2%, respectively. Then, three typical decision-making that decision-makers prioritize comfort, economy, and environmental impact are compared, and the set of alternative solutions is further shrunk. In short, the trade-off framework adopts the order of objective Pareto optimal and then subjective preference selection, narrowing the scope of alternatives for designers and saving time-cost of decision-making.

It should be mentioned that the output of the whole optimization process is based on a specific case, and it will vary depending on the user-defined variables, constraints, and objectives. Although the specific results of this research do not apply to other cases, the framework of this research is generalizable.

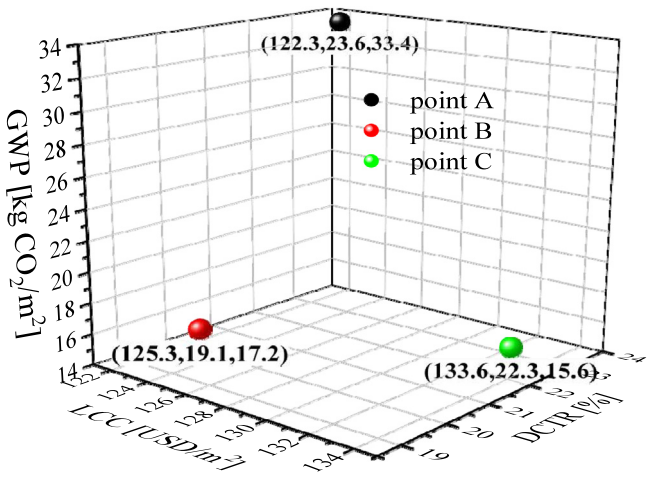

Fig. 10. The solution of three decision points.

CRediT authorship contribution statement

All authors read and contributed to the manuscript. **Ran Wang:** Model establishment, Data analysis and Paper writing. **Shilei Lu:** Methodology, Project administration, Supervision. **Wei Feng:** Validation and Writing. **Xue Zhai and Xinhua Li:** Collection of survey data.

Declaration of competing interest

The authors declare that they have no known competing financial interests or personal relationships that could have appeared to influence the work reported in this paper.

Acknowledgments

This research has been supported by the "National Key R&D Program of China" (Grant No. 2016YFC0700100).

The U.S. authors recognize Lawrence Berkeley National Laboratory's support from the U.S. Department of Energy under Contract No. DE-AC02-05CH11231 and support from the Energy Foundation, USA.

The U.S. Government retains a non-exclusive, paid-up, irrevocable, world-wide license to publish or reproduce the published form of this manuscript, or allow others to do so, for U.S. Government purposes.

All authors read and contributed to the manuscript.

References

Alajmi, A., Rodríguez, S., Sailor, D., 2018. Transforming a passive house a net-zero energy house: a case study in the Pacific Northwest of the US. Energy Conversion and Management. 172, 39–49.

Asadi, E., da Silva, M.G., Antunes, C.H., Dias, L., Glicksman, L., 2014. Multi-objective optimization for building retrofit: A model using genetic algorithm and artificial neural network and an application. Energy Build. 81, 444–456.

Ascione, F., Bianco, N., De Stasio, C., Mauro, G.M., Vanoli, G.P., 2016. Simulation-based model predictive control by the multi-objective optimization of building energy performance and thermal comfort. Energy Build. 111, 131–144.

ASHRAE, 2002. Guideline 14- 2002, Measurement of Energy and Demand Savings. American Society of Heating, Ventilating, Air Conditioning Engineers, Atlanta, Georgia.

ASHRAE, 2016. ANSI/ASHRAE Standard 55–2016. Thermal Environmental Conditions for Human Occupancy. ASHRAE Atlanta.

Bichiou, Y., Krarti, M., 2011. Optimization of envelope and HVAC systems selection for residential buildings. Energy Build. 43 (12), 3373–3382.

Bre, F., Roman, N., Fachinotti, V.D., 2020. An efficient metamodel-based method to carry out multi-objective building performance optimizations. Energy Build. 206.

Cabeza, L.F., Rincón, L., Vilariño, V., Pérez, G., Castell, A., 2014. Life cycle assessment (LCA) and life cycle energy analysis (LCEA) of buildings and the building sector: A review. Renew. Sustain. Energy Rev. 29, 394–416.

Carlucci, S., Bai, L., Dear, R.de., Yang, L., 2018. Review of adaptive thermal comfort models in built environmental regulatory documents. Build. Environ.

Chen, X., Huang, J., Yang, H., Peng, J., 2019. Approaching low-energy high-rise building by integrating passive architectural design with photovoltaic application. J. Clean. Prod. 220, 313–330.

Chen, X., Yang, H., 2017. A multi-stage optimization of passively designed high-rise residential buildings in multiple building operation scenarios. Appl. Energy 206, 541–557.

Chen, X., Yang, H., 2018. Integrated energy performance optimization of a passively designed high-rise residential building in different climatic zones of China. Appl. Energy 215, 145–158.

Chi, D.A., Moreno, D., Navarro, J., 2018. Correlating daylight availability metric with lighting, heating and cooling energy consumptions. Build. Environ. 132, 170–180.

China Building Materials Inspection and Certification Group, 2015. Green Building Material Selection Technology. Chemical Industry Press.

Ministry of Construction P R China, 2010. Design Standards for Energy Conservation of Residential Buildings in Cold and Cold Regions [M]. China Building Industry Press.

Ministry of Construction P R China, 2016. Standard for energy consumption of building GB51161-2016 (MOHURD).

Crawley, D.B., Lawrie, L.K., Winkelmann, F.C., Buhl, W.F., Huang, Y.J., Pedersen, C.O., et al., 2001. EnergyPlus: creating a new-generation building energy simulation program. Energy Build. 33 (4), 319–331.

D'Agostino, D., Parker, D., 2018. A framework for the cost-optimal design of nearly zero energy buildings (NZEBs) in representative climates across Europe. Energy 149, 814–829.

Deb, K., 2001. Multi-Objective Optimization using Evolutionary Algorithms. John Wiley & Sons.

Deb, K., 2015. Multi-objective evolutionary algorithms. In: Kacprzyk, J., Pedrycz, W. (Eds.), Springer Handbook of Computational Intelligence. Springer Berlin Heidelberg, Berlin, Heidelberg, pp. 995–1015.

Dutta, A., Samanta, A., Neogi, S., 2017. Influence of orientation and the impact of external window shading on building thermal performance in tropical climate. Energy Build. 139, 680–689.

Ellis, C.R., 2009. Who pays for green? The economics of sustainable buildings. EMEA Res. 19.

Feng, W., Zhang, Q., Ji, H., Wang, R., Zhou, N., Ye, Q., et al., 2019. A review of net zero energy buildings in hot and humid climates: Experience learned from 34 case study buildings. Renew. Sustain. Energy Rev. 114, 109303.

Fesanghary, M., Asadi, S., Geem, Z.W., 2012. Design of low-emission and energy-efficient residential buildings using a multi-objective optimization algorithm. Build. Environ. 49, 245–250.

Gagnon, R., Gosselin, L., Decker, S., 2018. Sensitivity analysis of energy performance and thermal comfort throughout building design process. Energy Build. 164, 278–294.

Glick, S., 2007. Life-Cycle Assessment and Life-Cycle Costs: A Framework with Case Study Implementation Focusing on Residential Heating Systems. Colorado State University.

Gou, S., Nik, V.M., Scartezzini, J.-L., Zhao, Q., Li, Z., 2018. Passive design optimization of newly-built residential buildings in Shanghai for improving indoor thermal comfort while reducing building energy demand. Energy Build. 169, 484–506.

Harkouss, F., Fardoun, F., Biwole, P.H., 2018. Passive design optimization of low energy buildings in different climates. Energy 165, 591–613.

Helton, J.C., Johnson, J.D., Sallaberry, C.J., Storlie, C.B., 2006. Survey of sampling-based methods for uncertainty and sensitivity analysis. Reliab. Eng. Syst. Saf. 91 (10–11), 1175–1209.

Huang, Y., J-l, Niu., T-m, Chung., 2012. Energy and carbon emission payback analysis for energy-efficient retrofitting in buildings—Overhang shading option. Energy Build. 44, 94–103.

Hurst, L.J., O'Donovan, T.S., 2019. A review of the limitations of life cycle energy analysis for the design of fabric first low-energy domestic retrofits. Energy Build. 109447.

IEA, Global Status Report for Buildings and Construction 2019. https://www.unenvironment.org/resources/publication/2019-global-status-report-buildings-and-construction-sector2018.

Islam, H., Jollands, M., Setunge, S., Haque, N., Bhuiyan, M.A., 2015. Life cycle assessment and life cycle cost implications for roofing and floor designs in residential buildings. Energy Build. 104, 250–263.

Jönsson, Å., Tillman, A.-M., Svensson, T., 1997. Life cycle assessment of flooring materials: case study. Build. Environ. 32 (3), 245–255.

Kheiri, F., 2018. A review on optimization methods applied in energy-efficient building geometry and envelope design. Renew. Sustain. Energy Rev. 92, 897–920.

Kirimtat, A., Krejcar, O., Ekici, B., Tasgetiren, M.F., 2019. Multi-objective energy and daylight optimization of amorphous shading devices in buildings. Solar Energy 185, 100–111.
Kovacic, I., Zoller, V., 2015. Building life cycle optimization tools for early design phases. Energy 92, 409–419.
Lamé, G., Leroy, Y., Yannou, B., 2017. Ecodesign tools in the construction sector: Analyzing usage inadequacies with designers' needs. J. Clean. Prod. 148, 60–72.
Lapisa, R., Bozonnet, E., Salagnac, P., Abadie, M.O., 2018. Optimized design of low-rise commercial buildings under various, climates - Energy performance and passive cooling strategies. Build. Environ. 132, 83–95.
Levy, S., Steinberg, D.M., 2010. Computer experiments: a review. ASTA-Adv. Stat. Anal. 94 (4), 311–324.
Lu, S., Wang, R., Zheng, S., 2017. Passive optimization design based on particle swarm optimization in rural buildings of the hot summer and warm winter zone of China. Sustainability. 9 (12), 2288.
Machairas, V., Tsangrassoulis, A., Axarli, K., 2014. Algorithms for optimization of building design: A review. Renew. Sustain. Energy Rev. 31, 101–112.
Mahapatra, K., 2015. Energy use and CO2 emission of new residential buildings built under specific requirements–The case of Växjö municipality, Sweden. Appl. Energy 152, 31–38.
Mearig, T., Coffee, N., Morgan, M., 1999. Life Cycle Cost Analysis Handbook: Draft: State of Alaska. Department of Education and Early Development.
Mechri, H.E., Capozzoli, A., Corrado, V., 2010. USE of the ANOVA approach for sensitive building energy design. Appl. Energy 87 (10), 3073–3083.
MOHURD, 1993. Code for Thermal Design of Civil Buildings (GB50176-93). China Planning Press, Beijing (in Chinese).
Mostavi, E., Asadi, S., Boussaa, D., 2017. Development of a new methodology to optimize building life cycle cost, environmental impacts, and occupant satisfaction. Energy 121, 606–615.
Nguyen, A.-T., Reiter, S., Rigo, P., 2014. A review on simulation-based optimization methods applied to building performance analysis. Appl. Energy 113, 1043–1058.
Ostergard, T., Jensen, R.L., Maagaard, S.E., 2018. A comparison of six metamodeling techniques applied to building performance simulations. Appl. Energy 211, 89–103.
Ouyang, X., Lin, B., 2014. Levelized cost of electricity (LCOE) of renewable energies and required subsidies in China. Energy Policy. 70, 64–73.
Pang, Z., O'Neill, Z., Li, Y., Niu, F., 2020. The role of sensitivity analysis in the building performance analysis: A critical review. Energy Build. 209.
Radford, A.D., Gero, J.S., 1980. On optimization in computer aided architectural design. Build. Environ. 15 (2), 73–80.
Rosso, F., Ciancio, V., Dell'Olmo, J., Salata, F., 2020. Multi-objective optimization of building retrofit in the Mediterranean climate by means of genetic algorithm application. Energy Build. 216.
Samuelson, H., Claussnitzer, S., Goyal, A., Chen, Y., Romo-Castillo, A., 2016. Parametric energy simulation in early design: High-rise residential buildings in urban contexts. Build. Environ. 101, 19–31.
Schmidt, M., Crawford, R.H., 2018. A framework for the integrated optimisation of the life cycle greenhouse gas emissions and cost of buildings. Energy Build. 171, 155–167.
Shi, X., Tian, Z., Chen, W., Si, B., Jin, X., 2016. A review on building energy efficient design optimization rom the perspective of architects. Renew. Sustain. Energy Rev. 65, 872–884.
Silva, A.S., Ghisi, E., 2014. Uncertainty analysis of the computer model in building performance simulation. Energy Build. 76, 258–269.
International Organization for Standardization, 2006. Environmental Management: Life Cycle Assessment; Requirements and Guidelines. ISO Geneva.
Tian, W., 2013. A review of sensitivity analysis methods in building energy analysis. Renew. Sustain. Energy Rev. 20, 411–419.
Wang, R., Lu, S., Feng, W., 2019. A three-stage optimization methodology for envelope design of passive house considering energy demand, thermal comfort and cost. Energy 116723.
Wu, X., Zhang, Z., Chen, Y., 2005. Study of the environmental impacts based on the "green tax"—applied to several types of building materials. Build. Environ. 40 (2), 227–237.
Yun, G.Y., Steemers, K., Baker, N., 2008. Natural ventilation in practice: linking facade design, thermal performance, occupant perception and control. Build. Res. Inf. 36 (6), 608–624.
Zhai, Y.N., Wang, Y., Huang, Y.Q., Meng, X.J., 2019. A multi-objective optimization methodology for window design considering energy consumption, thermal environment and visual performance. Renew. Energy 134, 1190–1199.
Zhu, L., Wang, B., Sun, Y., 2020. Multi-objective optimization for energy consumption, daylighting and thermal comfort performance of rural tourism buildings in north China. Build. Environ. 176.
Žigart, M., Lukman, R.K., Premrov, M., Leskovar, V.Ž., 2018. Environmental impact assessment of building envelope components for low-rise buildings. Energy 163, 501–512.
Zitzler, E., Deb, K., Thiele, L., 2000. Comparison of multiobjective evolutionary algorithms: Empirical results. Evol. Comput. 8 (2), 173–195.